COMMUNICATION

ChemComm www.rsc.org/chemcomm

1:1 Complexes of 5-(4-[*N*-*tert*-butyl-*N*-aminoxyl]phenyl)pyrimidine with manganese(II) and copper(II) hexafluoroacetonylacetonate†

Lora M. Field,[a] **Paul M. Lahti***[a] **and Fernando Palacio**[b]
[a] *Department of Chemistry, University of Massachusetts, Amherst MA 01003, USA.*
E-mail: lahti@chem.umass.edu
[b] *Instituto de Ciencia de Materiales de Aragón, CSIC – Universidad de Zaragoza, 50009, Zaragoza, Spain.*
E-mail: palacio@posta.unizar.es

Received (in Purdue, IN, USA) 7th December 2001, Accepted 24th January 2002
First published as an Advance Article on the web 25th February 2002

$Mn(hfac)_2$ and $Cu(hfac)_2$ form 1:1 complexes with 5-(4-[*N*-*tert*-butyl-*N*-aminoxyl]phenyl)pyrimidine that exhibit strong metal–nitroxide exchange; spin polarization models do not explain the antiferromagnetic exchange behavior between spin sites in these complexes.

An important and promising strategy for the development of hybrid organic–inorganic molecule-based magnetic materials is the coordination of paramagnetic ions with organic open-shell radicals and polyradicals.[1] In such systems, the exchange between the ion and the radical may be either ferromagnetic (FM) or antiferromagnetic (AFM), and still yield materials with net magnetic moments, so long as the spin quantum numbers of the building blocks are unequal. Here we report the crystallographic and preliminary magnetic studies of the coordination complexes formed between the stable radical 5-(4-[*N*-*tert*-butyl-*N*-aminoxyl]phenyl)pyrimidine (**1**) and $Mn(hfac)_2$ and $Cu(hfac)_2$.

Stable red radical **1** was synthesized as shown in Scheme 1, and reacted separately with one equivalent each of $Mn(hfac)_2$ and $Cu(hfac)_2$ in mixed solvent systems under slow crystallization conditions to give the 1:1 complexes **2** and **3** with good elemental analysis. The structures of these complexes were confirmed by X-ray crystallography.†‡ Over a period of months, there was no apparent decomposition of **2** or **3** when these were stored in the absence of strong light.

Fig. 1 shows ORTEP diagrams of **2** and **3**. Both are cyclic dimer type complexes in which the nitroxide spin site and one pyrimidine coordination site are complexed. Multiple efforts to make different complexes with molar ratios of **1**:$M(hfac)_2$ < 1.0 have failed to yield anything other than 1:1 complexes. In **2**, all of the Mn–O bond lengths are 2.10–2.30 Å; in **3**, the Cu–ON bond length is 2.40 Å, substantially longer than the other Cu–O bond lengths, 2.10–2.30 Å. The nitroxide Cu–ON bond is identifiably axial in **3**, and we consider the Mn–ON bond in **2** to be analogous, although the lower molecular symmetry of **2** makes harder a clear geometric differentiation of the equatorial and axial orientations. The interannular torsional angle in **2** is 29–30°, while that in **3** is 25°. There is substantial torsion about the nitroxide to phenyl N–C bond in both **2** (40°, 45°) and **3** (27°). The metal–metal distances within the complexes are fairly long: $r(Mn–Mn) = 10.4$ Å in **2**, $r(Cu–Cu) = 10.5$ Å in **3**. The inter-dimer metal–metal distances are shorter: the closest intermolecular $r(Mn–Mn) = 6.1$ Å in **2**, $r(Cu–Cu) = 8.2$ Å in **3**.

Dc magnetic susceptibility measurements were carried out on samples of **2** and **3** in a Quantum Design MPMS SQUID magnetometer over a range of 1.8–300 K at 1000 oersted (0.1 tesla). Fig. 2 shows plots of the corrected paramagnetic susceptibility χ as a function of absolute temperature T for each complex, as well as $1/\chi = f(T)$ (Curie–Weiss) plots of the same data.

Although **2** shows nearly linear Curie–Weiss behavior, **3** shows substantial deviation indicative of AFM interactions between spin sites. The high temperature limiting slopes of the Curie–Weiss plots are $C = 0.667$ and 0.977 emu K Oe^{-1} mol^{-1}, corresponding to $S = 2.12$ and 0.98 for **2** and **3**, respectively. In the case of **2**, this corresponds to $S \cong (5/2) - (1/2)$, or strong AFM exchange between the manganese ion and the nitroxide radical spin. For **3**, $S \cong (1/2) + (1/2)$, corresponding to a strong FM exchange between the copper ion and the nitroxide. The $T > 100$ K regions of the Curie–Weiss plots yield

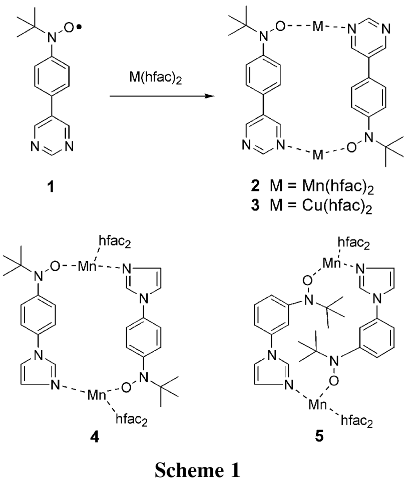

Scheme 1

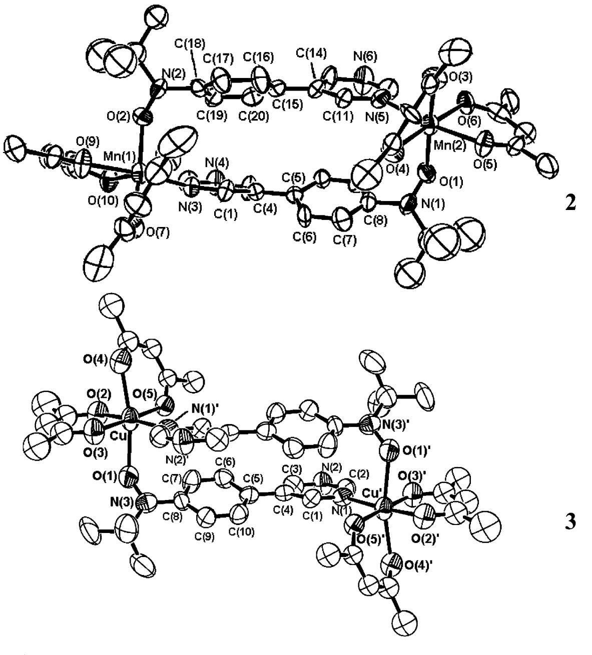

Fig. 1 ORTEP diagrams of **2** and **3**. Hydrogen and fluorine atoms are omitted for clarity.

---

† Electronic supplementary information (ESI) available: Spectroscopic data and crystallography for **1**. Fig. S1: ESR spectrum of **1**. See http://www.rsc.org/suppdata/cc/b1/b111295n/

DOI: 10.1039/b111295n

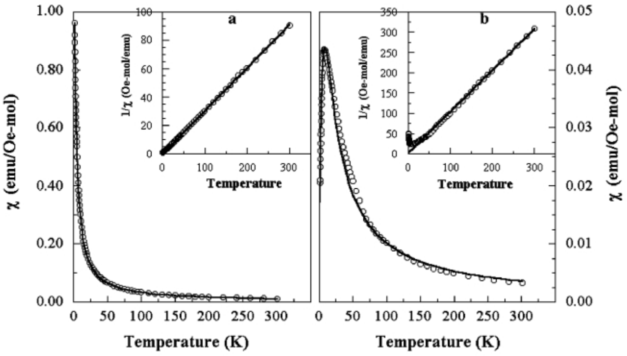

Fig. 2 Paramagnetic susceptibility (χ) *vs.* temperature plots for **2** and **3**, a and b, respectively. Inset figures show Curie–Weiss plots of $1/\chi$ *vs.* T for the same data.

Weiss constants of $\theta = -0.15$ K and -0.35 K for **2** and **3**, respectively.

It has been shown elsewhere that Mn–radical exchange is typically AFM in nature, while Cu–nitroxide exchange is typically FM when the coordination is axial.[1b,2] The strength of the M–NIT exchange interactions in **2** and **3** is notable. Based on the plots in Fig. 2, J/k(Mn–NIT) < -300 K and J/k(Cu–NIT) > 300 K. However, only for **3** are there significant interactions *between* the M–NIT spin sites.

Based on the crystal structures, it was assumed that the magnetic behaviors of **2** and **3** could be fitted to a Bleaney–Bowers dimer type model.[3] For **2**, we used the model described by Ishimaru *et al.*[4] for interactions between $S = 2$ spin sites. For **3**, we used Eqn. 1,

$$\chi = \frac{N_0 g_1 g_2 \mu_B^2}{k} \cdot \frac{\exp(-2J / kT)}{1 + 3\exp(-2J / kT)} \times \frac{1}{T - \theta} \qquad (1)$$

where J is the exchange coupling between M–NIT spin sites, g_1 and g_2 are g-factors of the different spin components, k is the Boltzmann constant, μ_B is the Bohr magneton constant, and θ is a mean field term. For **2**, $g_1 = g_2 = 2.00$ and $\theta = 0.0$ K was assumed, leading to an excellent fit for $\chi = f(T)$ with $2J/k = -0.45$ K. For **3**, satisfactory fitting required a non-zero mean-field field term. Fig. 2 shows the fit where $g_1 = 2.0$ and $g_2 = 2.2$, $\theta = -1.1$ K and $2J/k = -9.9$ K.

Despite an intermolecular approach of 6.7 Å between the Mn atoms in **2**, there is only a weak, AFM interaction between the Mn–NIT spin sites. By comparison, a twenty-fold larger AFM interaction is found in **3** as readily seen by the maximization and downturn of a χ *vs.* T plot at about 7 K. In an effort to rationalize the observed magnetic behavior, we compared our results to those for the structural analogue **4**, previously investigated by Ishimaru *et al.*[4] System **4** exhibits an upturn in magnetization, corresponding to a modest FM exchange interaction of $2J/k = +1.18$ K between strongly exchange linked, $S = 2$ Mn–NIT sites. By contrast, *meta*-linked **5** exhibited a downturn in magnetization corresponding to AFM exchange coupling between the Mn–NIT sites of $2J/k = -0.45$ K. The authors attributed the differing behavior to regiospecific intramolecular spin-polarization exchange effects transmitted through the organic radical π-systems, as in M–pyridyl–nitroxide complexes described elsewhere.[5] Although the exchange interactions in **4** and **5** could be attributed to through space effects, it is less obvious how to analyze these in structure–property terms.

Although systems **2** and **3** are connectivity analogues of **4**, they qualitatively show AFM instead of FM exchange. Possibly, spin polarization is stronger in **4** and **5** than in **2** and **3**. Solution ESR spectral analysis of **1**† shows no hyperfine coupling in the pyrimidine ring of > 0.1 G. Still, we hoped that coordination of the paramagnetic cations at the pyrimidine ring would induce spin polarization in the pyrimidine. If this is occurring, it is insufficient to induce the parity-expected FM exchange between the M–NIT spin sites within the dimer. As a result, **2** and **3** do not fit a regiospecific, intramolecular spin polarization model of exchange between M–NIT sites in the dimer. Also, the strength of exchange in **2** and **3** is not simply a function of the distance between M–NIT spin sites—the intramolecular distance is nearly the same, the intermolecular distance is smaller in **2**, but **3** shows the largest exchange effect. We think it likely that intermolecular mechanisms—or lack thereof—dominate exchange between the M–NIT spin sites in **2** and **3**, and we hope to report full details in the near future. Overall, despite the allure of spin-parity models to explain and predict exchange and magnetic behavior in molecular magnetic systems, the present work shows that such connectivity models do not invariably have predictive values. The models are useful guides, but not iron-clad rules.

This work was supported by the National Science Foundation (NSF CHE-9809548 and CHE-0109094), the Comision Interministerial de Ciencia y Tecnologia (CICYT-MAT2000-1388-C03-03), and the Fullbright España commission. The authors thank Dr. A. Chandrasekaran of the University of Massachusetts X-ray Structural Characterization Center (NSF CHE-9974648) for assistance with crystallographic analyses, and Dr. G. Dabkowski of the Microanalytical Laboratory for elemental analyses.

Notes and references

‡ For (**2**): mp 142–143 °C. Anal. Calcd. for $C_{24}H_{18}N_3O_5F_{12}Mn$: C, 40.04; H, 2.52; N, 5.84. Found: C, 40.28; H, 2.63; N, 5.64%. Dark red needles from ether/hexane. *Crystal data* for **2**: 0.50 × 0.15 × 0.05 mm, formula = $C_{24}H_{18}N_3O_5F_{12}Mn$, $M = 1422.71$, monoclinic, space group $P2_1/c$ (#14), $Z = 4$, $a = 9.888(9)$, $b = 28.922(5)$, $c = 21.273(1)$ Å, $\beta = 78.339(7)°$, $V = 5958.8(2)$ Å^3, $D_{calc} = 1.585$ g cm^{-3}, $T = 293$ K, λ(Mo-Kα) = 0.7107 Å, μ(Mo-Kα) = 0.557 mm^{-1}. 12102 Reflections were measured at an intensity threshold of $2\sigma(I)$. 6164 Independent reflections ($R_{int} = 0.1341$) were analyzed with 511 parameters using the program SHELXL-97. The final $wR(F^2)$ was 0.3377. The major source of disorder is in the CF_3 groups of the hfac ligands.

For (**3**): mp 132–134 °C. Anal. Calcd. for $C_{24}H_{18}N_3O_5F_{12}Cu$: C, 40.52; H, 2.55; N, 5.91. Found: C, 40.65; H, 2.48; N, 5.88%. Dark red plate from ether/hexane. *Crystal data* for **3**. 0.50 × 0.15 × 0.05 mm, formula = $C_{24}H_{18}N_3O_5F_{12}Cu$, $M = 1439.91$, monoclinic, space group $C2/c$ (#15), $Z = 4$, $a = 13.5050(2)$, $b = 14.5352(2)$, $c = 33.6543(5)$ Å, $\beta = 100.9537(5)°$, $V = 6485.91(16)$ Å^3, $D_{calc} = 1.475$ g cm^{-3}, $T = 293$ K, λ(Mo-Kα) = 0.7107 Å, μ(Mo-Kα) = 0.778 mm^{-1}. 10456 Reflections were measured at an intensity threshold of $2\sigma(I)$. 5710 Independent reflections ($R_{int} = 0.1280$) were analyzed with 382 parameters using the program SHELXL-97. The final $wR(F^2)$ was 0.3634. The major source of disorder is in the CF_3 groups of the hfac ligands. CCDC reference numbers are 178242–178244 for **1**–**3**. See http://www.rsc.org/suppdata/cc/b1/b111295n/ for crystallographic data in CIF or other electronic format.

1 (*a*) O. Kahn, *Molecular Magnetism*, VCH, New York, NY, 1993; (*b*) D. Gatteschi, in *Magnetic Properties of Organic Materials*, ed. P. M. Lahti, Marcel Dekker, New York, NY, 1999, p. 601ff; (*c*) *Molecular Magnetism: New Magnetic Material*, ed. K. Itoh and M. Kinoshita, Gordon & Breach, Amsterdam, The Netherlands, 2000, pp. 304–337; (*d*) H. Iwamura, K. Inoue and T. Hayamizu, *Pure Appl. Chem.*, 1996, **68**, 243.

2 H. Iwamura, in *Magnetic Properties of Organic Materials*, ed. P. M. Lahti, Marcel Dekker, New York, NY, 1999, pp. 641–644 and references therein.

3 B. Bleaney and K. D. Bowers, *Proc. R. Soc. London, Ser. A*, 1952, 214.

4 Y. Ishimaru, K. Inoue, N. Koga and H. Iwamura, *Chem. Lett.*, 1994, 1693.

5 (*a*) H. Iwamura and N. Koga, *Mol. Cryst. Liq. Cryst.*, 1999, **334**, 437; (*b*) M. Kitano, Y. Ishimaru, K. Inoue, N. Koga and H. Iwamura, *Inorg. Chem.*, 1994, **33**, 6012.